

# Fill the Void VII: A Continuing Study of the Impact of Solder Alloy on Voiding in Solder Joints.

Tony Lentz  
FCT Solder  
Windsor, CO, USA

## Abstract

This study is part of a series of papers on mitigation of voids in solder joints. Voiding is an ongoing concern for printed circuit board assembly (PCBA) manufacturers. As bottom terminated components (BTCs) become increasingly popular, the potential for voiding in solder joints has increased. Voiding limits are often imposed on PCBA manufacturers. These voiding limits lead manufacturers to find ways to mitigate voiding.

There are two major mechanisms for void formation. The first mechanism is gas entrapment in the solder joint. Gasses come from volatile materials in the flux, air gaps in the solder paste print, and from the PCB and components. The second mechanism for void formation is incomplete wetting or spread of the solder. When the solder alloy does not completely wet both the PCB pads and component leads, gaps remain in the solder joint.

This study is a continuation of work on voiding with respect to solder alloy and stencil design for quad-flat no-lead (QFN) components. The solder alloys tested include Sn63/Pb37, SAC305, SnBiCuNi, SnAgBiCu, and Sn37BiX. A water-soluble Pb-free solder paste flux and SAC305 reflow profile were used. The stencil design was varied on the QFN thermal pads to determine how gap size affects wetting of the solder alloy. Wetting behavior and gas entrapment were correlated to voiding for each solder alloy. The data for both parts of the study was summarized, and recommendations given to help “Fill the Void.”

## Introduction

Voiding in solder joints is a common issue for many PCBA manufacturers (Figure 1).

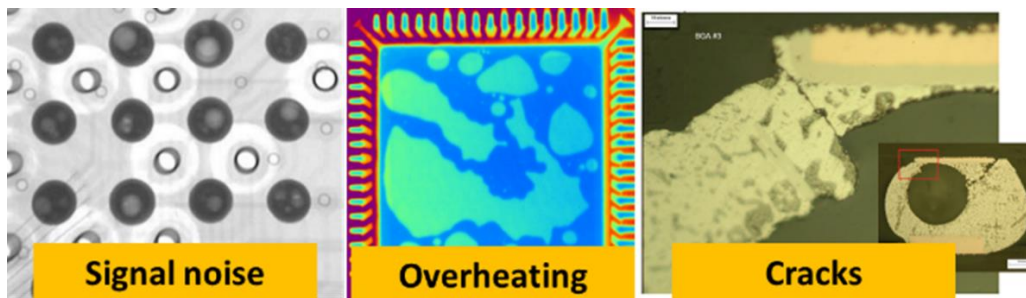


Figure 1. Voids in Solder Joints and Potential Defects.

Voids in solder joints can lead to signal noise, component overheating, and potentially cracks in the solder joints. These issues can also be caused by other sources. PCBA manufacturers often have void limits imposed by their customers, which may be tighter than limits from industry standards. Common void limits from IPC standards are shown below:

IPC J-STD-001H [1] & IPC-A-610G [2]

- 30% max area in BGAs
- 50% max area in QFN thermal pads

IPC-7093A BTCs [3]

- < 30% area typical on thermal pads (refer to J-STD-001 for limits)

IPC-7095C BGAs [4]

- < 25% area and < 50% diameter Class 1&2
- < 20% area and < 45% diameter Class 3

Void limits may have a connection to a history of solder joint failures or may be imposed as a safety factor to prevent possible failures. Regardless of the origin of the void limit, PCBA manufacturers are required to meet voiding limits which can be

46 challenging. There are many ways to mitigate voiding in solder joints, including modification of stencil design and using solder  
 47 alloys with low voiding potential.

48  
 49 Different solder pastes show dissimilar spread behaviors during reflow and have varied abilities to close gaps between the  
 50 printed solder paste bricks. Different solder pastes also show varied potential for gas generation and entrapment. Part of the  
 51 spreadability and gas entrapment of solder paste comes from the solder alloy portion of the solder paste which typically makes  
 52 up 85 to 90% by weight of the solder paste. Different solder alloys have individual metallurgical properties which contribute  
 53 to varied spread abilities and gas entrapment during reflow (Table 1).

54  
 55

**Table 1. Solder Alloy Properties.**

Property	Sn63/Pb37	SAC305	SnBiCuNi	SnAgBiCu	Sn37BiX	Measuring method
Melting Range (°C)	183	218-219	221-225	205-213	139-174	DSC : 2°C/min 30-300°C JISZ3198-1
Composition	Sn63/Pb37	Sn3Ag0.5Cu	Sn1.5Bi0.7CuNi	Sn3.5Ag3Bi1Cu	Sn37BiX	
Specific Gravity (g/cc)	8.4	7.4	7.4	7.5	8.1	@20°C
Tensile strength (MPa)	53	48	52	90	99	10mm/min @25°C
Elongation (%)	32	33	33	16	20	10mm/min @25°C
ε 0.2% (MPa)	16	41	39	61	81	10mm/min @25°C
Young's modulus (GPa)	32	51	56	55	47	JIS Z2280
Thermal expansion (ppm/K)	25	23	24	24	22	-40 - +150°C
Thermal conductivity (W/m·K)	50	58	54	53		Laser flush
Thermal mass (J/(kg·K))	150	219	224	232		Laser flush
Electric conductivity (μΩm)	0.14	0.14	0.14	0.16		4 terminal bridge

56  
 57  
 58  
 59  
 60

The stencil pattern used to print the solder paste plays a role in the spreadability of the solder paste. Webs are used in the stencil design for larger pads to break up the printed solder paste area into smaller bricks (Figure 2).

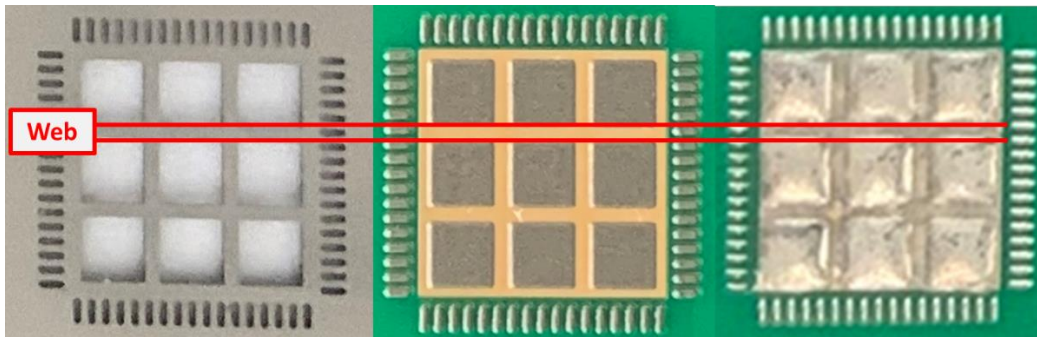


**Figure 2. Web Gaps in the Solder Paste Print for a QFN Thermal Pad.**

61  
 62  
 63  
 64  
 65  
 66  
 67  
 68  
 69

Webs in the stencil obviously create gaps in the solder paste print. Gaps in the solder paste print reduce the volume of solder paste which reduces the potential for float or skew of the component, and also reduces the risk of bridging between the thermal pads and input / output (I/O) pads. Web gaps also form gas escape routes which allow for volatile flux materials to escape minimize potential gas entrapment related voiding. In some cases, the stencil design creates gaps in the printed solder paste that are too wide or have too much area to successfully close during reflow. This leads to voiding in the solder joints.

70 Stencil manufacturers design stencils to optimize the solder paste print process with respect to certain defects, like insufficient  
 71 solder or bridging/shorting. Stencil manufacturers typically do not know which solder paste is being used, or the spreadability  
 72 of that solder paste. Therefore, the stencil design may create situations where the solder paste will not be able to completely  
 73 fill the gaps, resulting in high voiding in the solder joints.

74  
 75  
 76  
 77  
 78

The intent of this work was to vary the web (gap) widths in the printed solder paste for QFN thermal pads, and to determine how different solder alloys spread to fill those gaps. Different solder alloys also have different potential to trap gasses which affects voiding. Voiding in the solder joints was used as the primary metric to determine the ability of the solder alloy to release gasses and fill the gaps. The overall goal of this work is to find methods to “Fill the Voids” in solder joints.

79  
80  
81  
82  
83  
84  
85  
86  
87  
88  
89  
90  
91  
92  
93  
94  
95  
96  
97  
98  
99  
100  
101  
102  
103  
104  
105  
106  
107  
108  
109  
110  
111  
112  
113  
114  
115  
116  
117  
118  
119  
120  
121  
122  
123  
124  
125  
126  
127  
128  
129  
130  
131  
132  
133  
134  
135  
136

### *Prior Work*

Lentz and Smith [5] tested voiding in QFN thermal pad solder joints with 4 stencil designs including a standard 9-window pane, a diagonal window pane, a 5-dot pattern, and a diagonal stripe pattern. The area of coverage of printed solder paste was 65% of the thermal pad. Two solder pastes with SAC305 alloy and two reflow profiles were tested. The voiding was lowest for 3 of the 4 stencil designs while the others showed similar voiding levels. Voiding was lowest for one solder paste coupled with one reflow profile.

Lentz, Chonis, and Byers [6] studied voiding in QFN thermal solder joints with a host of variables. Some of the variables included several different solder pastes made with SAC305 alloy in type 3, 4, and 5 solder powder sizes, and two different solder powder manufacturers. 4 stencil designs were tested including a standard 9-window pane, a diagonal window pane, a 5-dot pattern, and a diagonal stripe pattern. The area of coverage of printed solder paste was ~65% of the thermal pad. Several reflow methods were tested including vapor phase with vacuum. Voiding was lower for some stencil designs, solder pastes, solder powder sizes, and some reflow methods. Vacuum reflow overcomes most of the other variables and resulted in very low voiding.

Lentz [7] analyzed voiding in QFN thermal pad solder joints with a large set of variables. Some of the variables were as follows:

- Solder alloy was varied including SAC305 alloy, SnCuNi alloy, SnBiCuNi alloy and a mixture of SAC305/SnBiCuNi alloys.
- QFN68s and QFN48s were used, and the stencil designs were varied for each. The area of coverage was 65% and 50% on the QFN68s and QFN48s respectively.
- Multiple stencil designs were used which varied the number of windows, window size and area of coverage. Web width was held constant at 8 mils.

Solder alloy influenced voiding, and the lowest voiding tended to be generated by the alloys with the widest melting ranges. Stencil design also had an impact on voiding, with higher area of coverage generating lower voiding levels.

Lentz and Smith [8] tested voiding for two sizes of QFN thermal pad solder joints with via hole in pad designs. A no clean solder paste with SAC305 alloy was used. Two via hole plugging methods were used and compared to open via holes as well as flat thermal pads with no via holes. The stencil designs included a standard 9 window pane with 65% area of coverage and a 20-mil web width, and a modified design which printed solder paste around the via holes and allowed for via gasses to escape, with 65% area of coverage and an 8-mil web width. Voiding was lower for the larger QFN68 than for the smaller QFN48 regardless of stencil design. Inclusion of open vias or partially tented vias in the thermal pad reduced overall voiding regardless of stencil design. Printing solder paste around the vias reduced the amount of flow of solder to the bottom of the PCBs and had a slight effect on reduction of voiding.

Smith and Lentz [9] studied voiding in solder joints for a variety of BTCs and varied the stencil design to minimize voiding. A commercially available no-clean SAC305 solder paste was used. Printed solder paste area of coverage on the thermal pads was varied from 50 to 80%. The stencil designs included largest web, standard web, largest perimeter, and most window panes. The web width, perimeter gap, and number of window panes were varied to achieve these stencil designs. Lower voiding was observed with higher area of coverage. The largest perimeter and the narrower web designs gave lower voiding levels. It should be noted that a quad-flat pack (QFP144) with a “belly” pad generated high levels of voiding regardless of stencil design, while the QFN voiding levels could be minimized through stencil design.

Lentz and Smith [10] revisited voiding in solder joints for a variety of BTC components. Stencil designs were varied including: 4 and 5 mil thick stencils, 60 and 70% area of coverage, and increasing the printed volume on QFN I/O perimeter pads. The web width was 20 mils, and the number of panes was kept at 4 for most of the components. Five different reflow profiles were used along with a no clean SAC305 solder paste. Voiding was lower for the 5-mil thick stencil, 70% area of coverage, and for the larger QFN sizes. As printed volume was increased on the QFN I/O perimeter pads, voiding decreased. In general, increasing the volume of solder paste on the thermal pads leads to less voiding.

Hillman, et. al., [11] studied how BTC voiding relates to component reliability. 4 solder alloys were tested including Sn63/Pb37, SAC305, and two high-reliability Pb-free alloys. Four different QFN's were daisy chained on a 10-layer test PCB which mimicked a real PCB. Thermal cycling was done from -55 to +125 °C for 3000 cycles. Failure rates were correlated to void area percentage (%). Sn63/Pb37 gave the lowest overall voiding levels, but this did not correlate to higher reliability. The Pb-free alloys had higher overall voiding levels, but again this did not indicate lower reliability. Overall, the correlation between voiding and reliability was very weak. A proposed voiding limit for thermal pads was given as established between the user

137 and manufacturer. When a limit is not established, then the soldered connection shall be larger than 50% of the thermal pad  
138 area, and this is a process indicator for Class 2 and 3 PCBs.

139  
140 Lentz [12] studied the impact of solder alloy on solder voiding with a no-clean Pb-free solder paste and a variety of solder  
141 alloys. Solder alloys showed different voiding levels in QFN thermalpad solder joints. Stencil web width was varied, and the  
142 voiding associated with certain alloys was affected by web width. A simple test measuring the time for gas bubbles to escape  
143 from the solder paste was conducted, and a correlation between mean void levels and gas escape time was found.

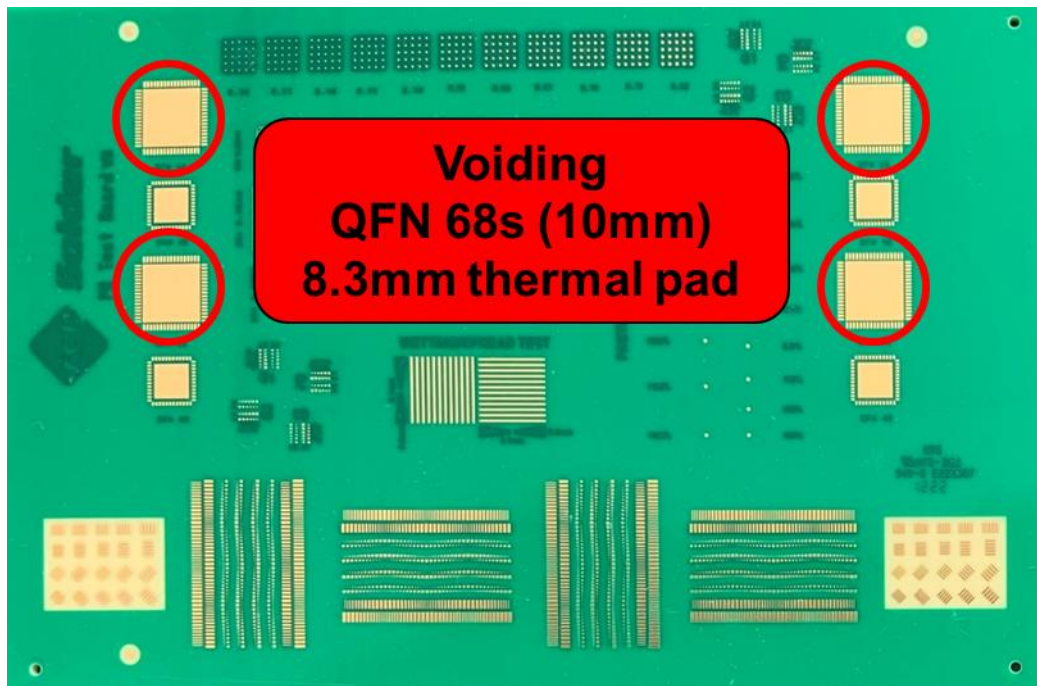
#### 145 **Experimental Methodology**

146 The goal of this work was to determine the effects of solder alloy coupled with stencil design on voiding in solder joints. The  
147 theory is that the leading causes of voiding are gas entrapment and incomplete wetting or spread of the solder alloy. There are  
148 many other factors that can influence voiding, so the experiment was designed to isolate solder alloy and stencil design as the  
149 only variables. This work was a continuation of previous work which used a no-clean Pb-free solder paste, and a variety of  
150 solder alloys [12]. For this work, a water-soluble Pb-free solder paste was chosen along with the same range of solder alloys.

151  
152 A commercially available water-soluble Pb-free solder paste flux was chosen, and a SAC305 reflow profile was run for  
153 comparison of all alloys. The solder alloys evaluated include: Sn63/Pb37, SAC305, Sn1.5Bi0.7CuNi (SnBiCuNi),  
154 Sn3.5Ag3Bi1Cu (SnAgBiCu) and Sn37BiX. SnBiCuNi is a silver-free alternative for SAC305, and both use the same reflow  
155 profile. SnAgBiCu is a high reliability alloy designed for automotive applications and typically reflows in a profile like  
156 SAC305. Sn37BiX is a low temperature, Pb-free alloy designed to reflow in a profile like a Sn63/Pb37 profile. The metal  
157 concentrations in the solder pastes were 89.5% by weight for Sn63/Pb37, and 88.3% by weight for all the Pb-free alloys. The  
158 solder powder size used was IPC type 4 (20-38  $\mu\text{m}$ ) for all alloys.

160 Solder paste reflow performance was evaluated using the PR test board V3 (Figure 3).

161

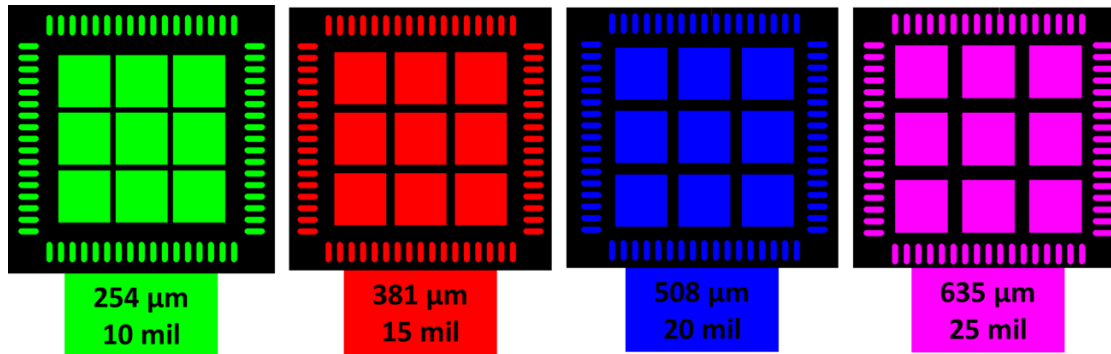


162  
163 **Figure 3. PR Test Board V3 from FCT Solder.**

164  
165 The PR test board V3 is made from 1.57 mm (0.062 in) thick FR-4 laminate with an electroless nickel immersion gold (ENIG)  
166 surface finish. This PCB was used to quantitatively measure wetting, solder balling, graping, and voiding in QFN68 thermal  
167 pads [13]. The QFN68 “dummy” components have a square 10 mm body size and an 8.3 mm square thermal pad.

168  
169 Wetting was measured as a spread test down a long circuit line, with increasing gap size between the printed solder paste bricks.  
170 As the solder spreads down the lines, the gaps between solder paste bricks close together, and fewer remaining gaps indicate  
171 good wetting. The number of gaps are counted and a percentage of wetting or spread is calculated. Solder balling is measured  
172 by evaluating random microscopic solder balling that occurs when solder paste pulls back from solder mask in pullback patterns  
173 that vary in size. Fewer random solder balls indicate good performance. Graping is measured using a range of very small

174 solder paste deposits on varying pad sizes and designs. The total number of graped solder deposits are counted and a graping  
 175 percentage calculated. Fewer solder deposits showing graping indicate good performance.  
 176  
 177 The normally used web width for the QFN68 thermal pad is 508-microns (20-mils) and the printed solder paste bricks are 2286-  
 178 microns (90-mils) square. The web width was varied to narrower and wider gaps from the norm. The stencil designs evaluated  
 179 included 4 different web widths: 254, 381, 508, and 635  $\mu\text{m}$  (10, 15, 20, and 25-mils respectively). Each stencil design had  
 180 the same area of coverage of solder paste on the thermal pad at 65%. The QFN68 thermal pad stencil designs are shown below  
 181 (Figure 4).  
 182



183  
 184 **Figure 4. QFN68 Thermal Pad Stencil Designs.**  
 185

186 Printing was performed on a commercially available solder paste printer. The printing process parameters are listed in Table  
 187 2 below.  
 188  
 189

**Table 2. Printing Process Parameters.**

Print speed (mm/sec)	30 mm/sec
Blade length (mm)	300 mm
Print pressure (kg)	5.0 kg
Separation speed (mm/sec)	3 mm/sec
Separation distance (mm)	1 mm
Stencil thickness ( $\mu\text{m}$ )	127 microns (5-mils)
Stencil material	Fine grain stainless steel

190  
 191 Reflow was performed in a commercially available 7-zone convection oven with an air atmosphere. The reflow profiles used  
 192 were linear ramp to spike (RTS) type profiles and the measured data is in Table 3 below.  
 193  
 194

**Table 3. Measured Reflow Profile Parameters.**

Parameter	SAC305 RTS	Sn63/Pb37 RTS	Sn37BiX RTS
Time Above Liquidus	57-59 sec > 220 °C	67-70 sec > 183 °C	75-77 sec > 174 °C
Peak Temperature	241-244 °C	208-210 °C	200-203 °C
Time from 25 °C to Peak	4.4-4.6 min	3.6-3.7 min	4.8-5.0 min

195  
 196 The SAC305 profile was used for the bulk of the testing. The Sn63/Pb37 reflow profile was run with the Sn63/Pb37 solder  
 197 paste and the 508-micron (20-mil) web, only on 1 test iteration for a comparison with the SAC305 profile. The Sn37BiX  
 198 profile was run with the Sn37BiX solder paste and the 508-micron (20-mil) web, only on 1 test iteration for a comparison with  
 199 the SAC305 profile. The SAC305 profile was run for all other solder paste and stencil combinations and the reflow profile  
 200 graph is in Figure 5.  
 201





Figure 5. Linear RTS Reflow Profile for SAC305.

Five solder pastes, each with the same water-soluble flux and a different alloy, were run with 4 stencil designs which gave a total of 20 combinations. 5 test boards were run for each solder paste and stencil combination, and 4 dummy QFN68 components were placed on each board. There were a total of 20 void measurements for each combination.

Voiding area % was evaluated using a 2D X-ray on the QFN68 thermal pad solder joints for each combination of solder paste and stencil design. Void area % data sets were compared using statistical analysis software. Tukey-Kramer means comparison with a 95% confidence level was used to determine significance of the differences in voiding.

A simple reflow test was conducted to measure the time between initial heating and the last gas bubble to escape the molten solder (Figure 6).

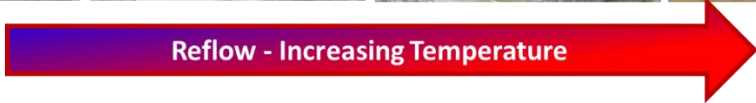
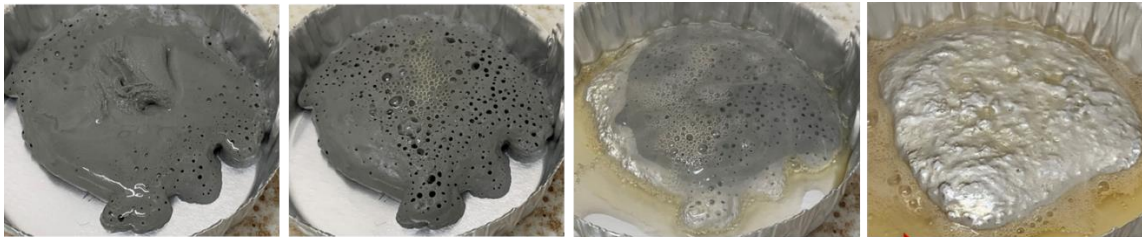


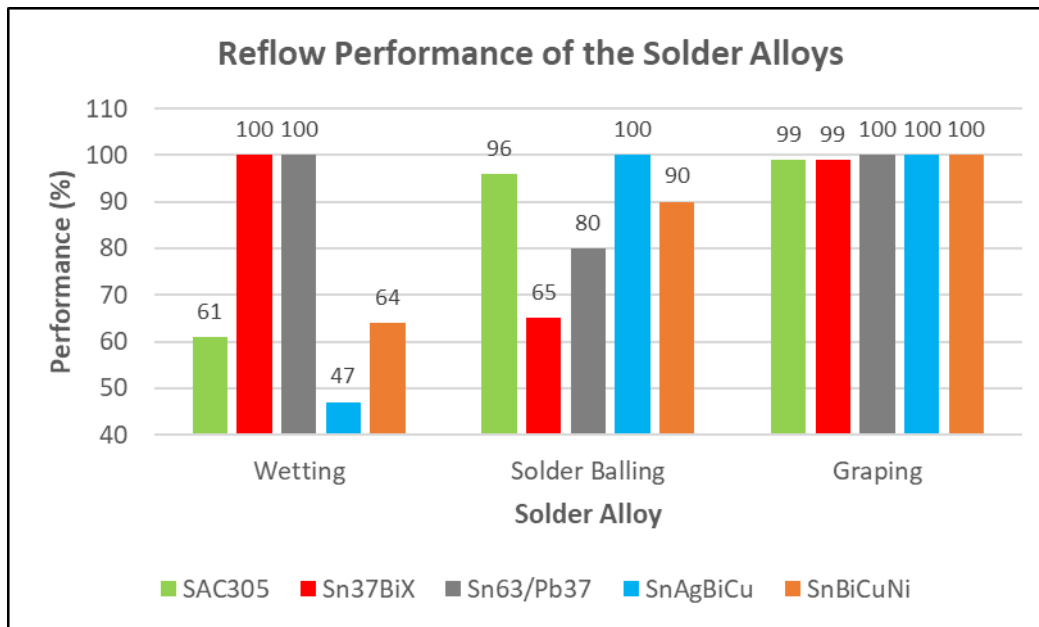
Figure 6. Solder Paste Melting and Gas Entrapment

Solder paste (20 +/- 0.2 grams) was placed in an aluminum weigh dish. The solder paste was heated on a hot plate at a temperature 60-70 °C above the melting point of the alloy. The hot plate temperature used for Sn63/Pb37 and Sn37BiX alloys was 250 °C. The hot plate temperature used for all other alloys was 280 °C. The time was measured between placement of the aluminum weigh dish on the hot plate and the last gas bubble escaping from the molten solder. The time for gas escape was correlated to the voiding levels from each solder alloy.

## Results

### Solder Paste Reflow Performance

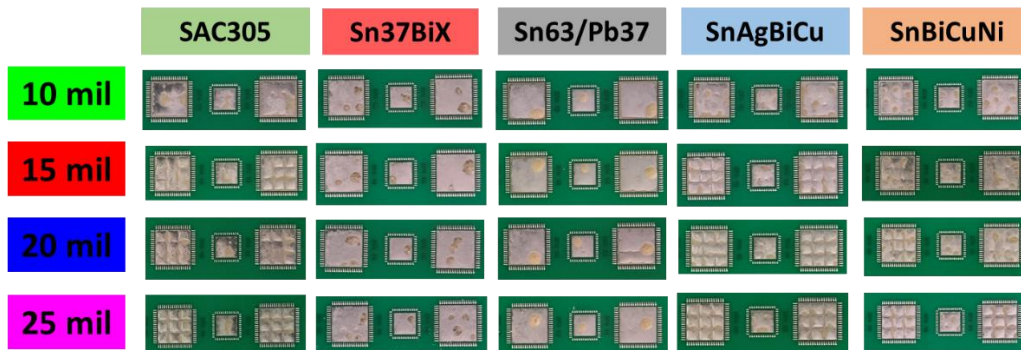
Wetting, solder balling, and graping performance were measured for the water-soluble solder paste and each solder alloy using the patterns on the PR test board run in the SAC305 reflow profile. These metrics were averaged from patterns on 2 test boards from each set of test boards. The results are reported as performance (%) for each solder alloy in Figure 7 below. Ideal performance is 100% in each category.



233 **Figure 7. Wetting, Solder Balling, and Graping Performance for Each Solder Alloy Using the SAC305 Reflow Profile.**

234  
235  
236 SnAgBiCu displayed the worst wetting on the PR test board, followed by SAC305 and SnBiCuNi. The best possible wetting  
237 was displayed by the Sn37BiX and Sn63/Pb37 alloys. Sn37BiX displayed the worst random solder balling, followed by  
238 Sn63/Pb37. SnBiCuNi and SAC305 displayed excellent / very low solder balling. The best possible solder balling was shown  
239 by SnAgBiCu alloy. Graping performance was near perfect for all the alloys. That is largely due to the water soluble Pb-free  
240 flux chosen to make the solder pastes, which is known to prevent graping.

241  
242 A bare board without QFN components was run for each solder paste and stencil combination in the SAC305 profile. Pictures  
243 of the QFN thermal pads were taken to compare solder spread behavior with respect to the gap sizes in the stencil design. The  
244 pictures are shown below (Figure 8).

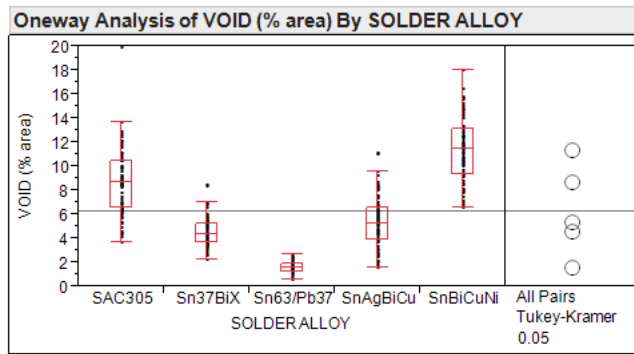


246 **Figure 8. Solder Spread in the QFN Thermal Pads for Each Solder Alloy and Gap Size.**

247  
248  
249 The Sn37BiX and Sn63/Pb37 alloys showed the best solder spread in the QFN thermal pads, with all gap sizes closed by the  
250 alloys. This matches the alloy performance on the PR test board wetting patterns. SAC305 and SnBiCuNi alloys showed near  
251 equivalent spread in the QFN thermal pads. The 10-mil gaps were closed, the 15-mil gaps were partially closed, and the larger  
252 gaps showed incomplete closure. This correlates to the wetting pattern data for these alloys. The SnAgBiCu alloy showed the  
253 worst solder spread on the QFN thermal pads, with only the 10-mil gaps closed by the alloy. Again, this matches what was  
254 observed in the PR test board wetting patterns.

255 *Voiding Performance*

256  
257  
258 Voiding data for the QFN thermal pad solder joints for the water-soluble solder paste was separated by solder alloy and is  
259 shown below (Figure 9). Each box plot includes all stencil gap widths. Ideal performance is 0% void area.



Excluded Rows 40

**Means Comparisons**

**Comparisons for all pairs using Tukey-Kramer HSD**

**Connecting Letters Report**

Level	Mean
SnBiCuNi A	11.4
SAC305 B	8.7
SnAgBiCu C	5.3
Sn37BiX C	4.5
Sn63/Pb37 D	1.6

Levels not connected by same letter are significantly different.

**Figure 9. Voiding by Solder Alloy Including all Stencil Gaps.**

261  
262  
263  
264  
265  
266  
267  
268  
269  
270  
271  
272  
273  
274  
275

SnBiCuNi gives the statistically highest voiding followed by SAC305, which gave higher voiding than the other alloys. SnAgBiCu and Sn37BiX showed similar voiding which was moderately low compared to the other alloys. The lowest overall voiding was shown by Sn63/Pb37. This ranking of void performance roughly correlates to wetting performance of the alloys, meaning poor wetting performance corresponds to higher voiding. The wetting of the alloys from worst to best is: SnAgBiCu, SAC305 = SnBiCuNi, Sn37BiX = Sn36/Pb37. The lower melting point alloys, Sn37BiX and Sn63/Pb37, showed the best overall wetting and the lowest voiding.

In the simple reflow test on a hot plate, the time from initial heating of the solder paste to the last gas bubble to escape the molten solder is in table 4 below. Also included is the mean void area (%) from Figure 9. The table is sorted from shortest time at the top to longest time at the bottom.

**Table 4. Time from Initial Heating until the Last Gas Bubble Escaped the Molten Solder and Mean Void Area.**

Solder Alloy	Time for Gas Bubble Escape (sec)	Mean Void Area (%)
Sn63/Pb37	120	1.6
Sn37BiX	160	4.5
SnAgBiCu	180	5.3
SAC305	220	8.7
SnBiCuNi	240	11.4

276  
277  
278  
279  
280  
281

Sn63/Pb37 alloy had the quickest gas escape time, followed by Sn37BiX and SnAgBiCu which had moderate gas escape times. SAC305 and SnBiCuNi had the longest gas escape times. This seems to correlate to mean voiding in QFN thermal pad solder joints. A graph was made (Figure 10) to correlate gas escape time to voiding area %. The mean void areas from Figure 9 were plotted against the gas escape time from Table 4.



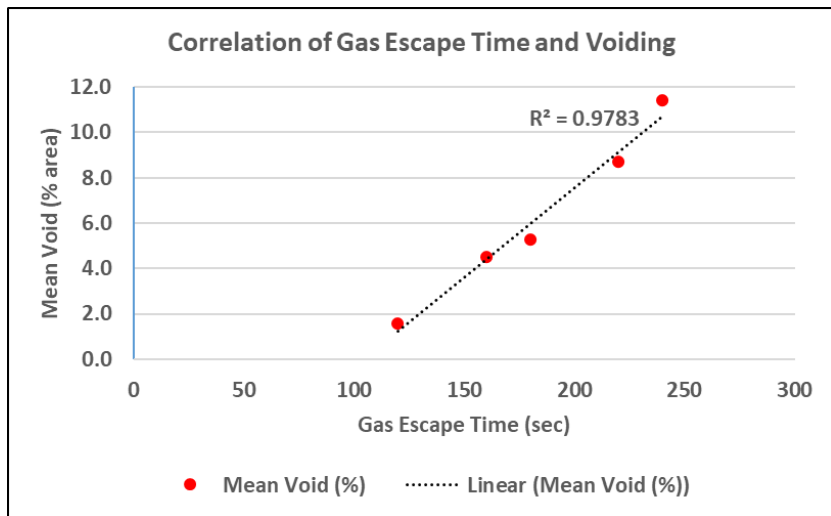
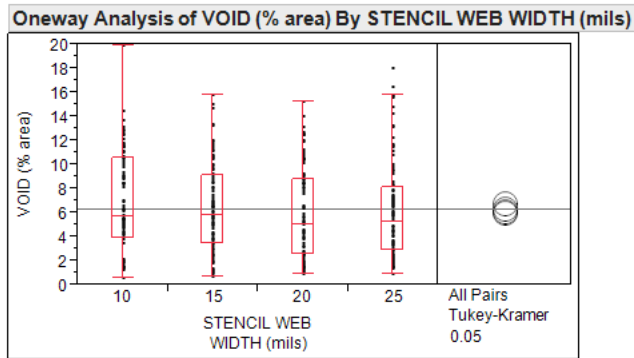


**Figure 10. Correlation of Gas Escape Time to Voiding.**

The gas escape time correlates linearly to voiding area % with an  $R^2$  value of 0.98. This simple gas escape time test may be a way to estimate the voiding potential due to gas entrapment for solder pastes.

Voiding data analysis broken out by stencil gap (web) width is shown below (Figure 11). Each box plot includes all solder alloys.



Excluded Rows 40

**Means Comparisons**  
**Comparisons for all pairs using Tukey-Kramer HSD**  
**Connecting Letters Report**

Level	Mean
10	A 6.7
15	A 6.3
25	A 6.1
20	A 6.0

Levels not connected by same letter are significantly different.

**Figure 11. Voiding by Stencil Web Width Including All Solder Alloys.**

This overall look at voiding by stencil gap width shows no statistical difference in voiding. A closer look at voiding by solder alloy broken out by web width gives a better understanding of the data.

Voiding by solder alloy broken out by web width is shown below (Figure 12).

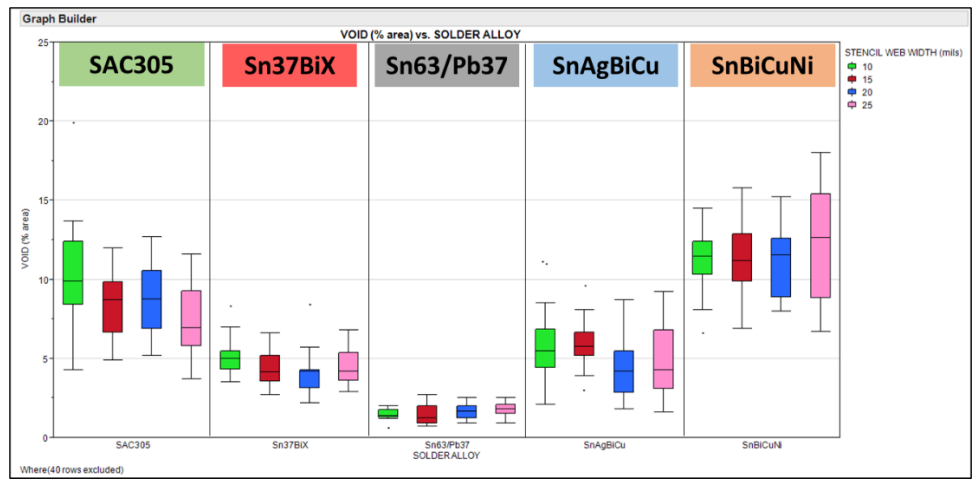


**Figure 12. Voiding by Solder Alloy Broken Out by Web Width.**  
**Green = 10 mil Web, Red = 15 mil Web, Blue = 20 mil Web, and Pink = 25 mil Web.**

299  
 300  
 301  
 302  
 303  
 304  
 305  
 306  
 307  
 308  
 309

SAC305 shows high voiding, but there seems to be a decreasing trend of voiding with increasing web width. Sn37BiX displays low voiding that doesn't vary much by web width. Sn63/Pb37 has the lowest overall voiding which doesn't vary by web width. SnAgBiCu shows moderate voiding that seems to decrease with increasing web width. SnBiCuNi displays the highest overall voiding and there is little influence by web width. Statistical analysis of voiding for each solder alloy broken out by web width is shown below (Figure 13).

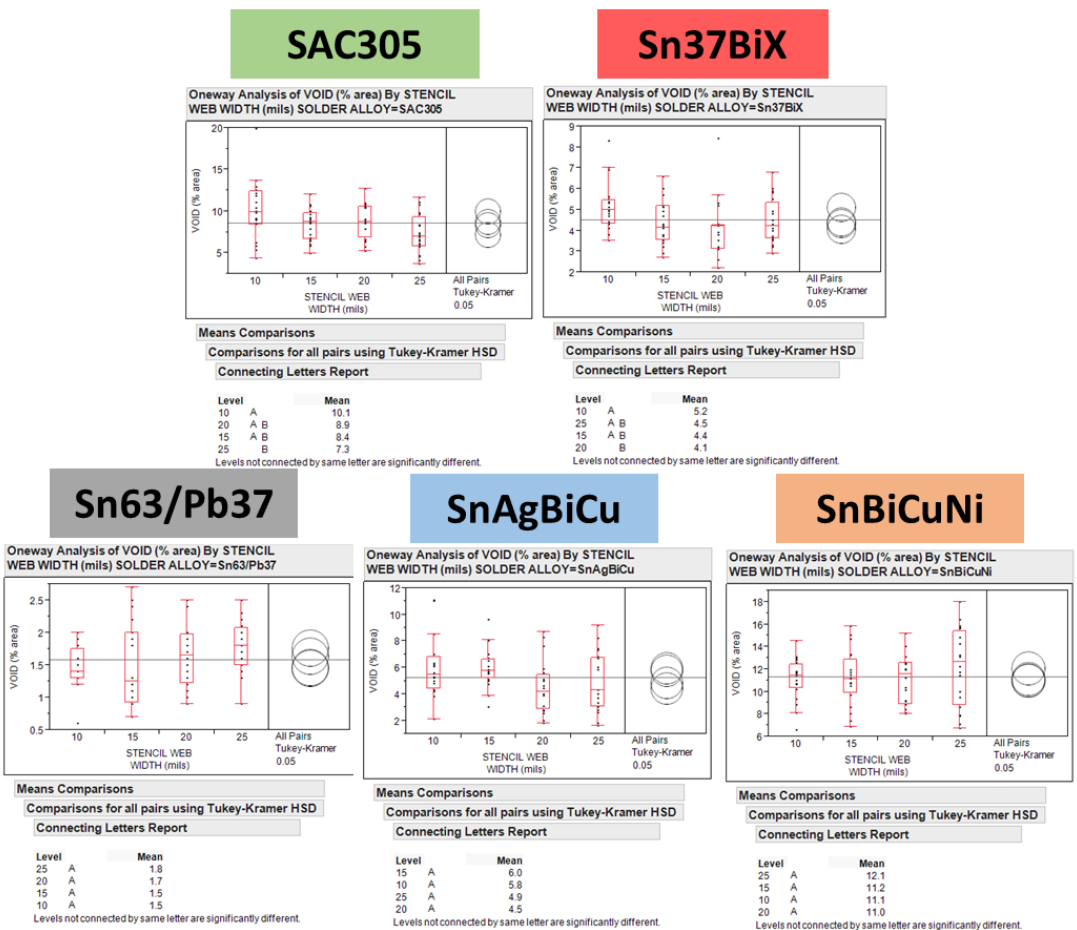
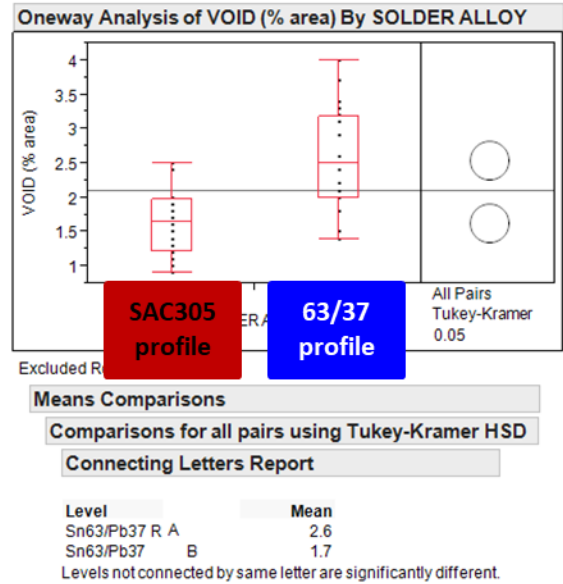


**Figure 13. Statistical Analysis of Voiding by Solder Alloy Broken Out by Web Width.**

310  
 311  
 312

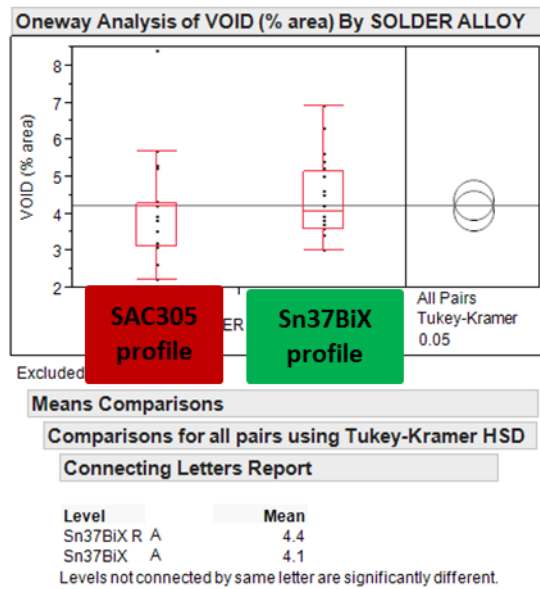
313 SAC305 alloy with the 10-mil web width has statistically higher voiding than the 25-mil web width. Sn37BiX shows a similar  
 314 trend with the 10-mil web width showing statistically higher voiding than the 20-mil web width. The voiding with the other  
 315 alloys is statistically similar for all web widths. This contradicts what was expected. Smaller gaps are theoretically easier to  
 316 close and therefore may show lower voiding, assuming the main cause of the voiding is poor wetting.  
 317  
 318 A comparison was made of voiding for Sn63/Pb37 solder alloy in the Pb-free SAC305 profile to a standard Sn63/Pb37 reflow  
 319 profile. The stencil with the 20-mil web width was used, and the mean void comparison is shown below (Figure 14).  
 320



321  
 322 **Figure 14. Voiding for the Sn63/Pb37 Solder Paste and the 20-mil Stencil Web,**  
 323 **Comparing the SAC305 Profile and Sn63/Pb37 Profile.**  
 324

325 Sn63/Pb37 alloy run in the Sn63/Pb37 reflow profile gave statistically higher voiding than running it in the SAC305 profile.  
 326 The water-soluble flux used to make the Sn63/Pb37 solder paste is normally used for Pb-free alloys and Pb-free reflow profiles.  
 327 The lower temperature Sn63/Pb37 reflow profile may have not fully evaporated the volatile materials from the flux which  
 328 could explain this difference in voiding.  
 329

330 A similar comparison of reflow profiles was done with Sn37BiX solder alloy. This low temperature Pb-free alloy was run in  
 331 a SAC305 profile and compared to a standard low temperature Pb-free (Sn37BiX) reflow profile and voiding was measured.  
 332 The stencil with the 20-mil web width was used for this comparison, and the mean void comparison is shown below (Figure  
 333 15).  
 334

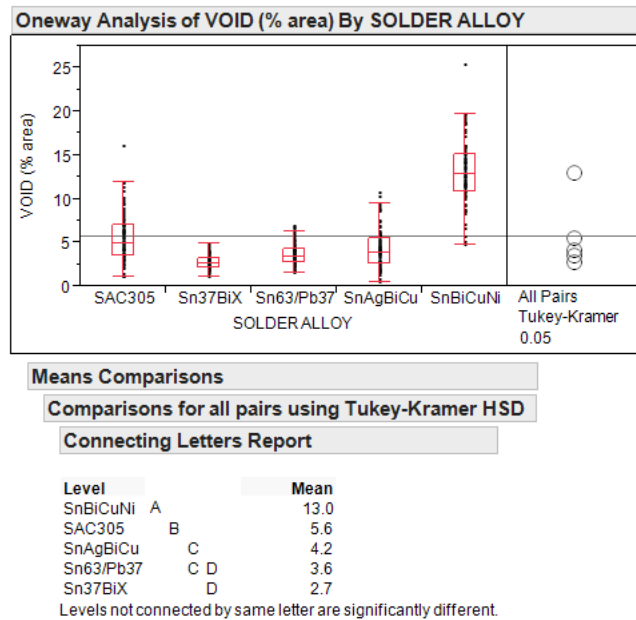


335  
336  
337  
338  
339 **Figure 15. Voiding for the Sn37BiX Solder Paste and the 20-mil Stencil Web,**  
340 **Comparing the SAC305 Profile and Sn37BiX Profile.**

341 Sn37BiX alloy run in the Sn37BiX reflow profile gave statistically similar voiding to the SAC305 profile. This is different  
342 than what was seen with the Sn63/Pb37 reflow profile comparison. The gas entrapment potential of these two alloys (Table 4)  
343 is different which may account for the differences in these reflow profile comparisons.

344 **Discussion**

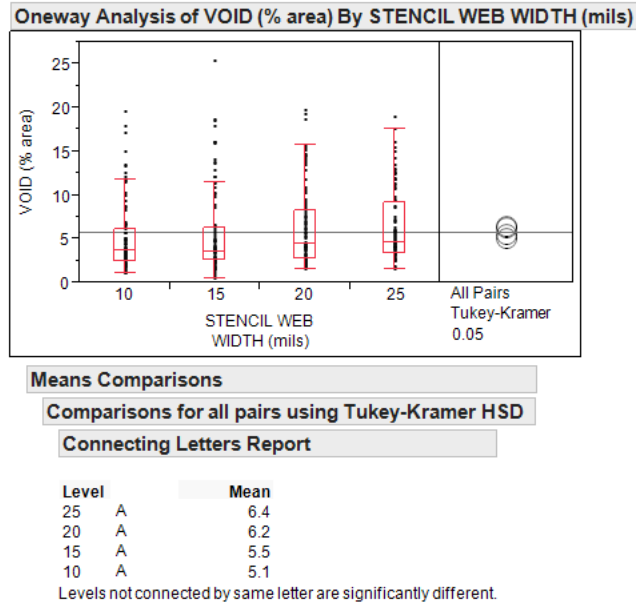
345 The prior work on determination of solder alloy influence on voiding [12] was conducted with a no-clean Pb-free solder paste  
346 flux and the same solder alloys used in this work. The results of the prior work are shown below for comparison of no-clean  
347 and water-soluble fluxes with these alloys. The voiding data sorted by solder alloy for the no-clean solder paste is shown in  
348 Figure 16 below.



349  
350 **Figure 16. Voiding by Solder Alloy from Previous Work with No-Clean Solder Paste.**

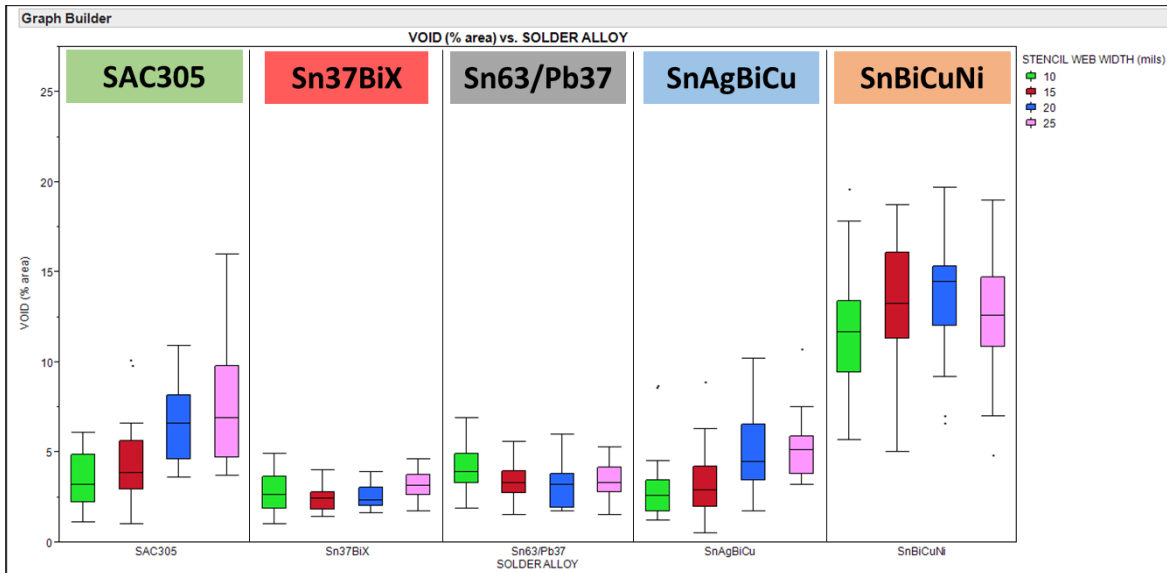
351  
352 Nearly the same order of voiding performance by alloy was seen with both water-soluble solder paste (Figure 9) and no-clean  
353 solder paste (Figure 16). The highest voiding was seen with SnBiCuNi followed by SAC305 which were significantly higher

354 than the other alloys. Lower voiding was found with the other 3 alloys. SnAgBiCu shows statistically higher voiding than the  
 355 Sn37BiX alloy, but Sn63/Pb37 alloy shows statistically similar voiding to these alloys.  
 356  
 357 Voiding by web width was also similar between the water-soluble flux (Figure 11) and no-clean flux (Figure 17).  
 358



359 **Figure 17. Voiding by Web Width from Previous Work with No-Clean Solder Paste.**

360  
 361  
 362 There is not a significant difference in voiding by web width when all solder alloys are averaged together for both the water-  
 363 soluble and no-clean solder pastes.  
 364  
 365 Breaking out voiding by both solder alloy and web width showed interesting results with the no-clean solder paste (Figure 18).  
 366

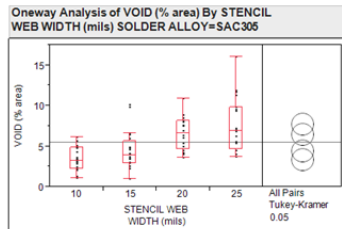


367 **Figure 18. Voiding by Alloy and Web Width from Previous Work with No-Clean Solder Paste.**  
 368 **Green = 10 mil Web, Red = 15 mil Web, Blue = 20 mil Web, and Pink = 25 mil Web.**

369  
 370  
 371 These results are a bit different for the no-clean solder paste than what was found with the water-soluble solder paste (Figure  
 372 12). The Tukey-Kramer statistical analysis for the no-clean solder paste is shown below (Figure 19).  
 373  
 374



## SAC305

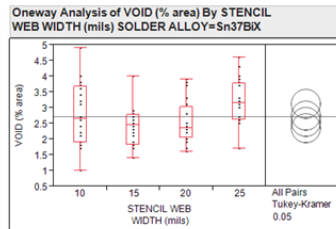


Means Comparisons  
Comparisons for all pairs using Tukey-Kramer HSD  
Connecting Letters Report

Level	Mean	
25	A	7.8
20	A	6.5
15	B	4.5
10	B	3.4

Levels not connected by same letter are significantly different.

## Sn37BiX

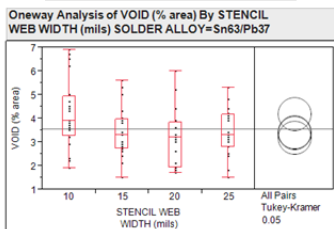


Means Comparisons  
Comparisons for all pairs using Tukey-Kramer HSD  
Connecting Letters Report

Level	Mean	
25	A	3.2
10	A B	2.8
20	A B	2.6
15	B	2.4

Levels not connected by same letter are significantly different.

## Sn63/Pb37

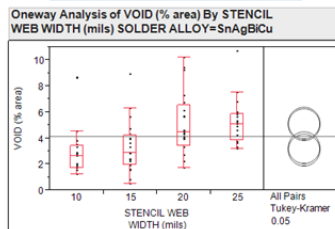


Means Comparisons  
Comparisons for all pairs using Tukey-Kramer HSD  
Connecting Letters Report

Level	Mean	
10	A	4.2
15	A B	3.4
25	A B	3.4
20	B	3.2

Levels not connected by same letter are significantly different.

## SnAgBiCu

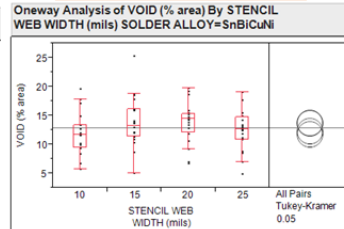


Means Comparisons  
Comparisons for all pairs using Tukey-Kramer HSD  
Connecting Letters Report

Level	Mean	
25	A	5.2
20	A	5.1
15	B	3.3
10	B	3.1

Levels not connected by same letter are significantly different.

## SnBiCuNi



Means Comparisons  
Comparisons for all pairs using Tukey-Kramer HSD  
Connecting Letters Report

Level	Mean	
20	A	13.8
15	A	13.8
25	A	12.4
10	A	11.9

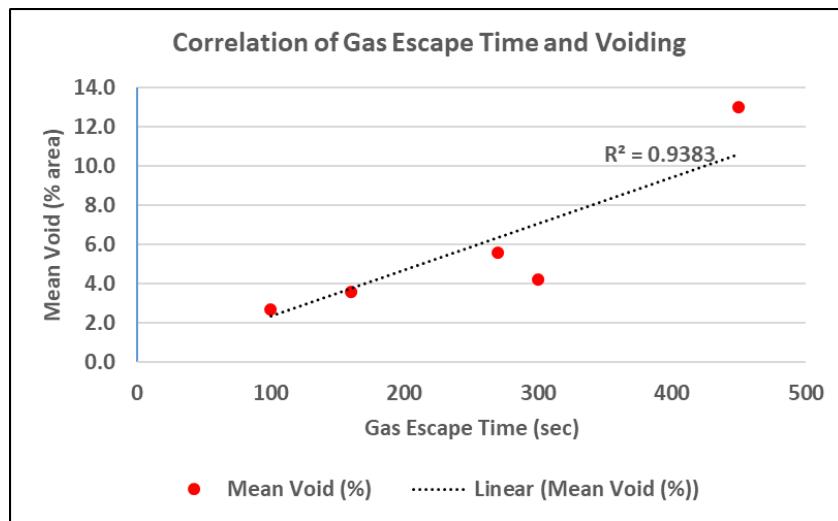
Levels not connected by same letter are significantly different.

Figure 19. Statistical Analysis of Voiding by Solder Alloy Broken Out by Web Width from Previous Work with No-Clean Solder Paste.

375  
376  
377  
378  
379  
380  
381  
382  
383  
384  
385  
386  
387  
388

SAC305 shows increasing voiding with increasing web width for the no-clean solder paste, but the opposite is true with the water-soluble solder paste (Figure 13). Sn37BiX and Sn63/Pb37 show randomly different results for voiding by web width for the no-clean and water-soluble solder pastes. SnAgBiCu shows increasing voiding with increasing web width for the no-clean solder paste, but statistically similar voiding for each web width and the water-soluble solder paste. SnBiCuNi shows similar high voiding which does not vary by web width for both the no-clean and water-soluble solder pastes. It is apparent that the solder paste flux plays a role in the wetting and gas entrapment potential of these solder alloys.

The simple test of measuring time for gasses to escape from the molten solder was correlated to mean void % in previous work with the no-clean solder paste (Figure 20).



389  
390 **Figure 20. Correlation of Gas Escape Time to Voiding from Previous Work with No-Clean Solder Paste.**  
391

392 The time for gas to escape from molten solder vs. mean void (% area) shows a linear correlation for both water-soluble (Figure  
393 10) and no-clean solder pastes (Figure 20). This data suggests that gas escape time may be a good predictor of voiding in QFN  
394 thermal pads for both no-clean and water-soluble solder pastes.  
395

### 396 **Conclusions and Recommendations**

397 Solder alloy plays a role in voiding in QFN thermal pad solder joints. There are significant differences in voiding between  
398 solder alloys when compared using the same solder paste flux and the same processing conditions. The ability of a solder alloy  
399 to wet and fill gaps has a correlation to voiding. Stencil gap width influenced voiding for some solder alloys, but not for others.  
400 Alloys which spread better tend to give lower voiding in QFN thermal pad solder joints. The solder paste flux influences both  
401 voiding and wetting. Solder paste fluxes and solder alloys are not the only sources of voiding in solder joints, and other factors  
402 may overcome their influence on voiding.  
403

404 If voiding in solder joints is a concern, then the reader should be aware that changing solder alloys may change voiding  
405 performance which can cause voiding limits to be exceeded. If one can specify a solder alloy, then it is recommended to choose  
406 an alloy which gives low voiding potential in the solder paste that is used. Minimizing gaps in the solder paste print also aids  
407 in reduction of voiding potential for some solder pastes and alloys. These recommendations are intended to help the reader to  
408 “Fill the Void.”  
409

### 410 **Acknowledgements**

411 The author gives thanks to Greg Smith with BlueRing Stencils, who provided the stencils used in this work.  
412

### 413 **References**

- 414 [1] J-STD-001 Task Group (5-22a), “Requirements for Soldered Electrical and Electronic Assemblies”, IPC J-STD-001H,  
415 September 2020.  
416 [2] IPC-A-610 Task Group (7-31b), “Acceptability of Electronic Assemblies”, IPC-A-610G, October 2017.  
417 [3] Bottom Termination Component (BTC) Task Group (5-21h), “Design and Assembly Process Implementation for Bottom  
418 Termination Components (BTCs)”, IPC-7093A, October 2020.  
419 [4] Ball Grid Array (BGA) Task Group (5-21f), “Design and Assembly Process Implementation for BGAs”, IPC-7095C,  
420 January 2013.  
421 [5] Lentz, Smith, “Fill the Void”, Proceedings of SMTA International, 2016.  
422 [6] Lentz, Chonis, Byers, “Fill the Void II: An Investigation into Methods of Reducing Voiding”, Proceedings of IPC Apex  
423 Expo, 2017.  
424 [7] Lentz, “Fill the Void III”, Proceedings of SMTA International, 2017.  
425 [8] Lentz and Smith, “Fill the Void IV: Elimination of Inter-Via Voiding”, Proceedings of IPC Apex Expo, 2018.  
426 [9] Smith and Lentz, “Root Cause Stencil Design for SMT Component Thermal Lands”, Proceedings of SMTA International,  
427 2019.  
428 [10] Lentz and Smith, “Fill the Void V - Mitigation of Voiding for Bottom Terminated Components”, Proceedings of IPC Apex  
429 Expo, 2020.  
430 [11] Hillman, et. al., “Bottom Terminated Component (BTC) Void Concerns: Real and Imagined”, Proceedings of SMTA  
431 International, 2019.

- 432 [12] Lentz, "Fill the Void VI: A Study of the Impact of Solder Alloy on Voiding in Solder Joints", Proceedings of SMTA  
433 International, 2023.
- 434 [13] Lentz, "The Effects of Surface Finish on Solder Paste Performance - The Sequel", Proceedings of SMTA International,  
435 2019.
- 436